

X-Ray Photoelectron Study of Lanthanide Borosilicate Glass

K. I. Maslakov^a, S. V. Stefanovsky^b, A. Yu. Teterin^a, Yu. A. Teterin^a, and J. C. Marra^c

^aRussian Research Centre "Kurchatov Institute," pl. Kurchatova 1, Moscow, 123182 Russia

e-mail: teterin@ignph.kiae.ru

^bState Unitary Enterprise of the City of Moscow—United Ecology, Technology, and Research Center on RAW Conditioning and Environmental Protection (SUE SIA "Radon"), Sed'moi Rostovskii per. 2/14, Moscow, 119121 Russia

e-mail: profstef@mtu-net.ru

^cSavannah River National Laboratory, Savannah River Site, Building 773-42A, Aiken, SC 29808 United States

Received May 12, 2008

Abstract—The elemental and ionic quantitative analyses of the synthetic lanthanide borosilicate glass (Al–B–Gd–Hf–La–Nd–Pu–Si–Sr–O) are performed using the characteristics of the X-ray photoelectron spectra of the outer-shell and inner-shell electrons in the binding energy range 0–1000 eV. The oxidation states of the metal ions in this glass are determined and correspond to the Al³⁺, La³⁺, Nd³⁺, Gd³⁺, Hf⁴⁺, Pu⁴⁺, Si⁴⁺, and Sr²⁺ ions. Taking into account the binding energies of the O 1s electrons for the glass sample under investigation, the average lengths of metal–oxygen bonds on the surface of the sample are estimated to be 0.191 and 0.176 nm, which correspond to oxygen binding energies of 531.3 and 532.3 eV, respectively.

DOI: 10.1134/S1087659609010039

INTRODUCTION

Actinides are the most dangerous components of high-level wastes because of their long half-lives and the high chemical and radioactive toxicity. Their immobilization and long-term storage require matrices with a high chemical durability and radiation resistance. At present, borosilicate glasses and titanate or titanate zirconate ceramic materials have been considered to be suitable materials for the use as matrices for these purposes [1]. To date, the vitrification of high-level wastes from radiochemical plants of the United States and the Western Europe with the formation of borosilicate-based glasses (aluminophosphate-based glasses in Russia) has been the only process implemented on an industrial scale. Therefore, this technology has also been considered from the standpoint of its applicability to immobilization of wastes with a high content of actinides, in particular, plutonium. A great deal of research in the design, synthesis, and analysis of the properties of actinide-containing glasses and ceramic materials has been performed in the framework of the international program on the nonproliferation of the fissile materials and the disposition of the excess weapons plutonium [2].

The main problem associated with the development of glasses for immobilization of actinide wastes is that, in silicate and borosilicate glasses, oxides of transuranium elements, primarily, plutonium, have a low solubility, which depends substantially on their oxidation state and the ionic radius. The solubility decreases with a decrease in the charge and the radius of the actinide ion, i.e., in the series $An(VI) > An(V) > An(III)$ and $Th, U(IV) > Np(IV) > Pu(IV)$ [3]. Correspondingly, the

solubility in silicate-based glasses is maximum for UO₃ and minimum for PuO₂, AmO₂, Am₂O₃, and Cm₂O₃. The maximum concentration of PuO₂ in homogeneous borosilicate glasses does not exceed 2 wt % [4], and the individual PuO₂ phase is formed at higher concentrations.

The studies performed at the Savannah River National Laboratory (United States) resulted in the development of the lanthanide borosilicate glass with a PuO₂ content of up to ~9.5 wt % [5, 6]. However, detailed investigations with the use of X-ray powder diffraction analysis and electron microscopy revealed that this glass contains residual unreacted plutonium dioxide. The purpose of this study was to determine the oxidation states of plutonium and other elements in the glass under consideration.

X-ray photoelectron spectroscopy is one of the advanced methods for determining the oxidation state of elements. In our earlier work [7], we investigated borosilicate glasses containing up to ~7 wt % U.

SAMPLE PREPARATION AND EXPERIMENTAL TECHNIQUE

The lanthanide borosilicate glass (LaBS) of the calculated composition (mol %) 11.4Al₂O₃, 21.8B₂O₃, 4.4Gd₂O₃, 3.9HfO₂, 6.8La₂O₃, 5.2Nd₂O₃, 4.5PuO₂, 39.1SiO₂, and 2.9SrO (the contents of the components in wt % are given in the table) was prepared as follows. A plutonium nitrate solution was mixed with a 2 M sodium hydroxide solution. A plutonium hydroxide precipitate was calcined to the formation of PuO₂, which was ground in an agate mortar. The other oxides were

Composition of the lanthanide borosilicate glass sample per La atom according to the results of calculations and X-ray photoelectron spectroscopic data and electron binding energies E_b of the main lines

Oxide	Oxide content, wt %	Relative composition		E_b for ions M_{nlj} , eV		E_b for oxides, eV [8, 10]
		Calculation	X-ray photoelectron spectroscopy			
Al ₂ O ₃	9.0	1.67	1.24	Al 2 <i>p</i>	73.8	4.3
B ₂ O ₃	11.8	3.19	–	B 1 <i>s</i>	–	191.4
Gd ₂ O ₃	12.2	0.63	0.60	Gd 3 <i>d</i> _{5/2}	1187.8	1187.3
HfO ₂	6.3	0.29	0.38	Hf 4 <i>d</i> _{5/2}	213.2	213.4
La ₂ O ₃	17.2	1.00	1.00	La 3 <i>d</i> _{5/2}	835.6 (839.1)	835.1 (838.6)
Nd ₂ O ₃	13.6	0.76	0.89	Nd 3 <i>d</i> _{5/2}	978.5 (982.4)	(978.0) 981.9
PuO ₂	9.5	0.32	0.25	Pu 4 <i>f</i> _{7/2}	426.5	426.6
SiO ₂	18.1	2.84	3.00	Si 2 <i>s</i>	153.5	153.8
SrO	2.3	0.21	0.22	Sr 3 <i>d</i> _{5/2}	134.2	132.4

Note: The electron binding energies were measured with respect to the energy of the C 1*s* electrons of hydrocarbons on the surface of the sample $E_b = 285.0$ eV and with respect to the line width at half-height $\Gamma = 1.3$ eV. The broadened oxygen line is observed at $E_b = 531.8$ eV with $\Gamma = 2.1$ eV. The electron binding energies for lines with lower intensities are given in parentheses.

mixed, and the prepared mixture was treated in an AGO-2U planetary mill, which made it possible to produce powders with a developed specific surface area and a high reactivity. The mechanically activated powder was carefully mixed with the PuO₂ powder, and the mixture in a closed platinum tube was heated at a rate of 10°C/min to a temperature of 1500°C, held at this temperature for 30 min, and cooled to room temperature. The prepared product was milled, repeatedly heated to a temperature of 1500°C, and held for 1 h. Cooling resulted in the formation of a visually homogeneous greenish vitreous material, which was investigated using X-ray powder diffraction on a DRON-4 diffractometer (Fe radiation) and X-ray photoelectron spectroscopy.

The X-ray photoelectron spectra of the samples under investigation were recorded at room temperature on an MK II VG Scientific electrostatic spectrometer with the use of Al*K*_α and Mg*K*_α X-ray radiation at a residual pressure of 1.3×10^{-7} Pa. The spectrometer resolution measured as the width at half-height of the line of the Au 4*f*_{7/2} electrons was equal to 1.2 eV. In this paper, the electron binding energies E_b (eV) are given with respect to the energy (taken equal to 285.0 eV) of C 1*s* electrons of hydrocarbons on the surface of the sample. The errors in the measurement of the binding energies and widths of the lines of electrons were equal to 0.1 eV, and the errors in the measurement of the relative intensities were 10%. In the table, the line widths Γ (eV) at half-height are presented with respect to the width $\Gamma(\text{C } 1s) = 1.3$ eV in order to compare them with the data of other investigations [8]. Samples for measurements of the X-ray photoelectron spectra were prepared from the finely dispersed powder ground in the

agate mortar in the form a dense thick layer pressed into the surface of a double-sided adhesive tape.

The elemental and ionic quantitative analyses of the surface of the sample under investigation were performed taking into account that the intensities of the spectral lines are proportional to the ion concentrations in the sample. In our work, these analyses were carried out using the relationship $n_i/n_j = (S_i/S_j)(k_j/k_i)$, where n_i/n_j is the relative concentration of the atoms to be analyzed, S_i/S_j is the relative intensity (area) of the lines of the inner shell electrons of these atoms, and k_j/k_i is the experimental relative sensitivity factor. In our work, these factors with respect to carbon were as follows: 1.00 (C 1*s*), 2.64 (O 1*s*), 0.24 (B 1*s*), 0.74 (Al 2*p*), 0.92 (Al 2*s*), 24.0 (La 3*d*_{5/2}), 8.0 (La 4*d*), 5.68 (Hf 5*d*_{5/2}), 16.8 (Nd 3*d*_{5/2}), 8.0 (Nd 4*d*), 44.0 (Pu 4*f*_{7/2}), 12.0 (Gd 3*d*_{5/2}), 8.0 (Gd 4*d*), 1.08 (Si 2*p*), 1.04 (Si 2*s*), and 5.92 (Sr 3*d*) [9]. The X-ray photoelectron spectra of the sample under investigation were interpreted using the characteristics of the corresponding spectra for the Al₂O₃, La₂O₃, Gd₂O₃, Nd₂O₃, SiO₂ [8, 10], SrO [11], and PuO₂ [12] oxides (see table).

RESULTS

X-Ray Powder Diffraction Analysis

The prepared sample, for the most part, is amorphous. However, this sample contains traces of crystalline phases of the britholite La_{7.58}(Si_{1.05}O₄)₆O₂: (JCPDS no. 76-0338, see also, no. 75-1145) and PuO₂ (JCPDS no. 41-1170) type (Fig. 1). The angular positions, the interplanar distances, and the intensities of the reflections of both phases somewhat differ from the refer-

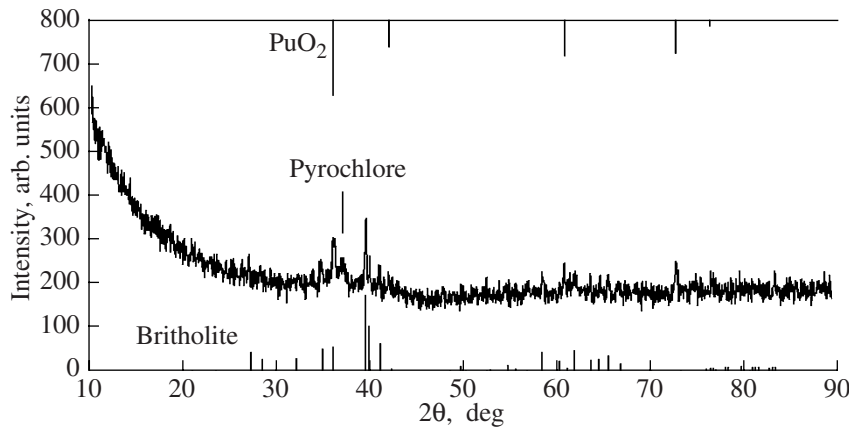


Fig. 1. X-ray diffraction pattern of the LaBS glass.

ences data involved in the JCPDS–ICCD database, because their actual chemical compositions do not coincide with stoichiometric compositions. In particular, the britholite phase can contain heavier lanthanides and even plutonium [13].

X-Ray Photoelectron Spectra

The X-ray photoelectron spectra of the studied ceramic samples in the electron binding energy range 0–1000 eV contain lines corresponding to the elements entering into the composition of the ceramic material under consideration. This energy range can be conventionally divided into three parts [8]. In the first electron binding energy range from 0 to 15 eV, the spectra exhibit a structure predominantly associated with the electrons of the outer valence molecular orbitals (OVMOs), which, for the most part, are formed by the electrons of open atomic valence shells. In the second electron binding energy range from 15 to 50 eV, the structure in the spectra is predominantly determined by the electrons of the inner valence molecular orbitals (IVMOs) and associated with the electrons of the low-energy completely filled valence shells of neighboring atoms. The characteristics of this structure reflect the structure of the nearest environment of the ion under consideration in the compound [8]. In the third range from 50 eV to higher energies, there arises a spectral structure determined by the inner (core) electrons, which make a weak contribution to the formation of inner molecular orbitals. This is almost ignored in the interpretation of X-ray photoelectron spectra. However, in this range, there can arise a structure associated with the spin–orbit interaction characterized by the splitting ΔE_{sl} (eV), multiplet splitting ΔE_{ms} (eV), multielectron excitations, dynamic effects, etc. Since the parameters of this structure characterize different properties of compounds, they are used in investigations in the combination with traditional characteristics, such as the electron binding energy, the chemical shifts of levels

and the differences between them, and the intensities of spectral lines [12].

Spectra of Low-Energy Electrons (from 0 to 50 eV)

In the low-energy range, the spectrum of the glass sample under investigation exhibits structures of the electrons of the outer valence molecular orbitals with maxima at 2.4, 5.8, and 9.4 eV due to the $Ln 4f^n$, $Ln 5d$, $Ln 6s$, etc., and O $2p$ outer valence electrons (where Ln is a lanthanide), as well as structures of the electrons of the inner valence molecular orbitals determined by the $Ln 5s$, $Ln 5p$, Hf $4f$, etc., and O $2s$ electrons (Fig. 2). The maxima at 18.2 and 23.4 eV in the binding energy range of the $Ln 5p$, Hf $4f$, and O $2s$ electrons are most pronounced. In actual fact, the bands of the inner valence molecular orbitals rather than individual lines are observed in the range of the electrons of the inner valence molecular orbitals. Unfortunately, the structures

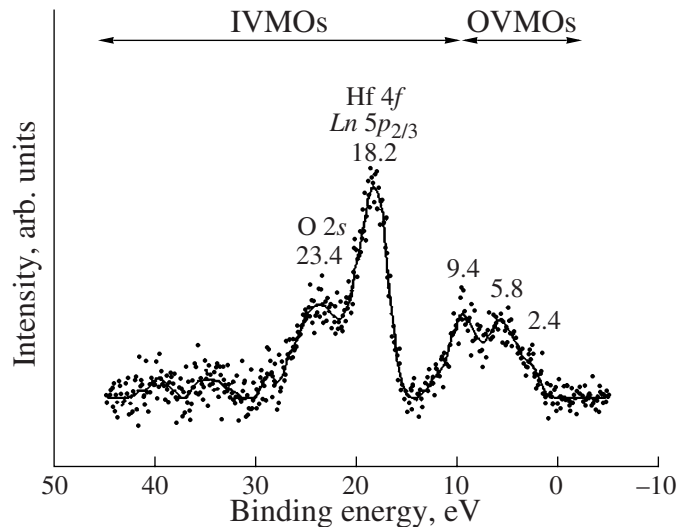


Fig. 2. X-ray photoelectron spectrum of low-energy electrons of the LaBS glass.

of these spectra allow us to perform only the qualitative elemental analysis, because the spectra under consideration represent not individual atomic lines but systems of molecular orbitals. In this energy range, the spectra contain only the lines characteristic of the compounds of the aforementioned elements.

Spectra of Inner Electrons (from 50 to 1000 eV)

When the elemental and ionic quantitative analyses of samples are carried out using X-ray photoelectron spectroscopy, it is common practice to use the most intense lines of elements entering into the sample composition [8–10]. However, important characteristics for the determination of the oxidation state of *Ln 4f* and *An 5f* transition elements of lanthanides and actinides are parameters of the fine structure of lines [8, 12]. For example, the multiplet splitting of the lines of the *Ln 4s* and *Ln 5s* electrons is proportional to the number of unpaired *Ln 4f* electrons in lanthanide ions, which enables one to determine uniquely their oxidation and spin states. In turn, the structure of “shake up” satellites in the spectra of *Ln 3d* and *An 4f* electrons provide information on the oxidation state of ions and the ionic character of bonds [8, 12].

For the glass sample under consideration, we chose the lines of the Al *2s*, Al *2p*, B *1s*, *Ln 3d*, *Ln 4d*, Hf *4d*, Pu *4f*, Si *2s*, Sr *3d*, and O *1s* electrons (table, Fig. 3). Unfortunately, reliable spectra of the *Ln 4s* electrons could not be obtained as a result of a low intensity of the corresponding lines. If spectra of different elements overlap with each other, as is the case with the lines of the *Ln 5p* electrons (Fig. 3), it is possible to use other lines that are more characteristic, as, for example, the line of the *Ln 3d* electrons (Fig. 3). The spectra of the C *1s* electrons contain the main line at 285.0 eV and also the line with a low intensity at 288.6 eV, which should be attributed to CO₃²⁻ carbonate groups on the surface of the sample. It follows from these spectra that a nonuniform charging of the sample, which leads to a distortion of the line shape in spectra, is almost absent.

The spectra of the Al *2p*, Hf *4d*, Si *2s*, and Sr *3d*_{5/2} electrons are observed in the form of single lines (table). The spectrum of the B *1s* electrons is not observed because of the small photoionization cross section for these electrons. In this respect, the initial boron content in the sample is taken into account in the discussion of the data of the quantitative analysis. The spectrum of the O *1s* electrons is represented in the form of a symmetric broadened line at 531.8 eV, which can be decomposed into two components with electron binding energies of 531.3 and 532.3 eV (Fig. 3c).

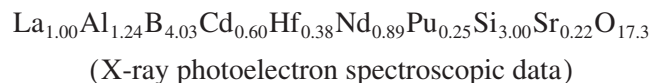
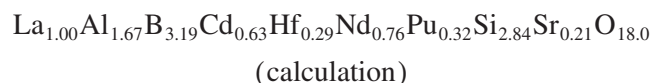
The spectra of the *Ln 3d* electrons in the sample under investigation consist of spin doublets (ΔE_{sl}) and satellites associated with the many-electron excitations (Figs. 3a, 3b). The analysis of the binding energies of the *Ln 3d* electrons and the satellite shape permits us to make the unique inference that the lanthanide ions in

the sample under investigation are characterized by the oxidation state *Ln*³⁺. As for the La₂O₃ oxide [8], the spectrum of the La *3d* electrons of the sample under investigation in the range of higher binding energies with respect to the main doublet lines exhibit shake up satellites with $\Delta E_{sat}(\text{La } 3d_{5/2}) = 3.5$ eV and the relative intensity $I_{sat}/I_0 = 86\%$ (Fig. 3, table). The intensities of these satellites correlate with the ionic character of the La–O chemical bond in the sample. The enhancement of the ionic character of the chemical bond leads to a decrease in the intensity of the satellites under consideration [8]. The structure of the spectrum of the Nd *3d*_{5/2} electrons in the glass sample contains the shake up satellite with $\Delta E_{sat}(\text{Nd } 3d_{5/2}) = 3.9$ eV and the relative intensity $I_{sat}/I_0 = 73\%$, which is considerably lower than that in the spectrum of these electrons in the Nd₂O₃ oxide (Fig. 3b, table). This indicates that the ionic character of the Nd–O bond differs from that in the Nd₂O₃ oxide. The spectra of the Gd *3d*_{5/2} electrons are observed in the form of a single broadened line at 1187.8 eV with a low intensity (table).

The spectrum of the Pu *4f* electrons involves two components due to the spin–orbit interaction with the splitting $\Delta E_{sl} = 12.5$ eV (Fig. 3d). The binding energies of these electrons are in good agreement with those for the PuO₂ oxide (table). This suggests that plutonium ions in the samples under investigation, for the most part, are in the Pu⁴⁺ state.

Qualitative and Quantitative Elemental and Ionic Analyses

The atomic composition of the surface layer of the glass sample under investigation per lanthanum atom was determined from the line intensities (areas) with due regard for the experimental relative sensitivity factors [9]. The atomic composition obtained is as follows (table):



The sample composition in weight percent of oxides is also presented in the table.

One of the factors responsible for the increase in the error in the determination of the quantitative composition of samples is an inaccuracy in the measurement of the areas of the lines in the X-ray photoelectron spectra at low concentrations of elements (the sensitivity of the method is ~0.1–1.0 wt % of compound). As was noted above, the difference between the X-ray photoelectron spectroscopic and calculated data is associated with the fact that the spectroscopic data reflect the surface composition, which can differ from the composition of the sample bulk.

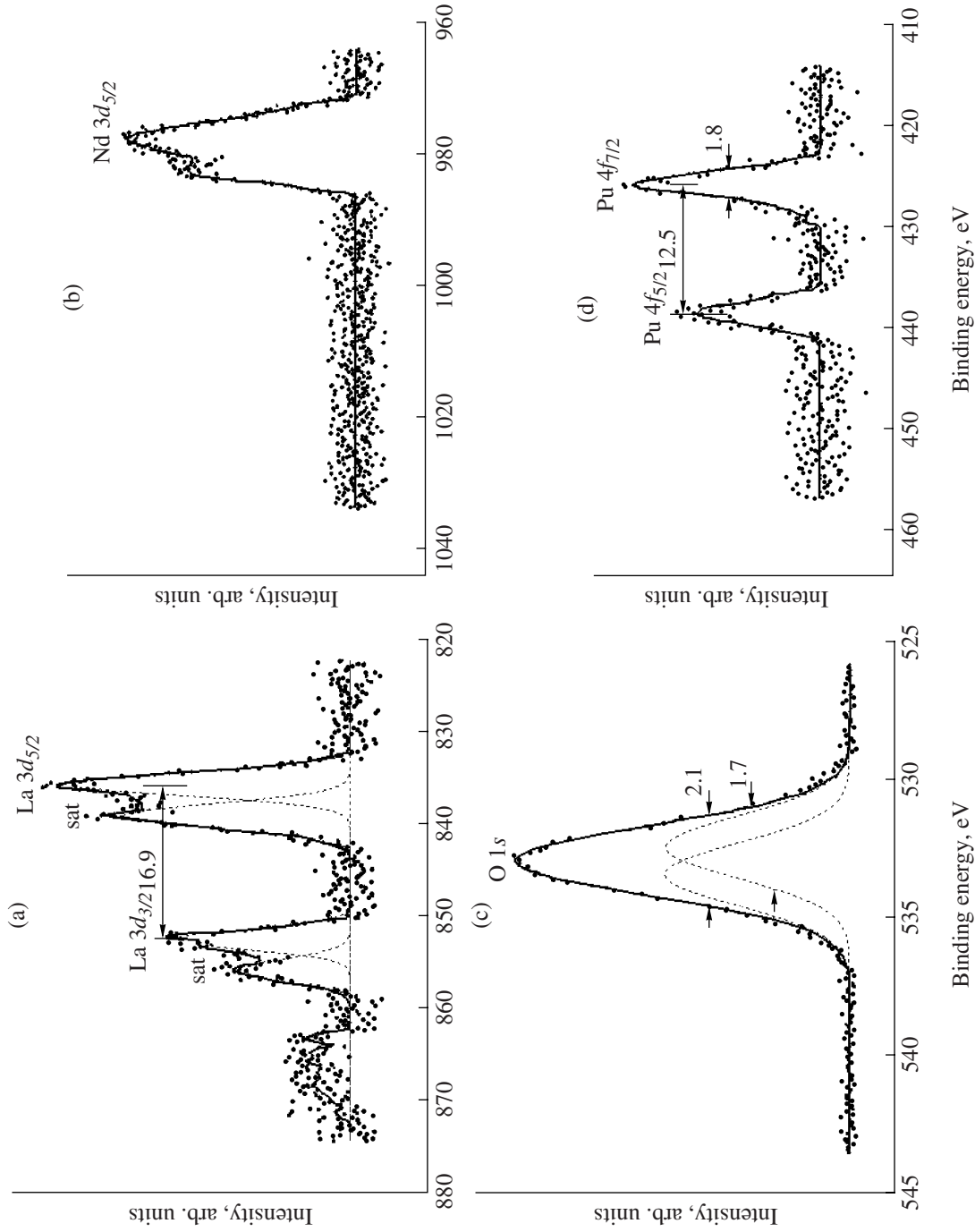


Fig. 3. X-ray photoelectron spectra of the (a) La 3d, (b) Nd 3d_{5/2}, (c) O 1s, and (d) Pu 4f electrons for the LaBS glass.

Determination of the Metal–Oxygen Bond Lengths

The spectrum of the O 1s electrons of the sample under investigation consists of a broad line with a maximum at 531.8 eV, which can be represented as the superposition of two lines at 531.3 and 532.3 eV with the widths $\Gamma(\text{O } 1s) = 1.3$ eV (Fig. 3c). By using the relationship

$$E_b(\text{eV}) = 2.27R_{M-O}^{-1}(\text{nm}) + 519.4, \quad (1)$$

derived in [11], we obtain

$$R_{M-O}(\text{nm}) = 2.27(E_b - 519.4)^{-1}, \quad (2)$$

This means that the metal–oxygen bond lengths R_{M-O} (nm) can be estimated from the binding energy of the O 1s electrons. These bond lengths on the surface of the sample under investigation are estimated to be 0.191 and 0.176 nm.

DISCUSSION OF THE RESULTS

Almost all elements in the glass under investigation are characterized by their typical oxidation states and occur in the form of Al^{3+} , La^{3+} , Nd^{3+} , Gd^{3+} , Hf^{4+} , Si^{4+} , and Sr^{4+} ions. Plutonium can be in several oxidation states, of which the states Pu(IV) and Pu(III) are most typical of glasses and ceramic materials [3, 4, 14–17]. Upon synthesis in the air atmosphere, the average formal valence of plutonium is +3.75 (75% Pu^{4+} , 25% Pu^{3+}) in zirconolite and is close to +4 in borosilicate glasses, which is in good agreement with the data obtained in our work.

In contrast to the spectra of plutonium-containing glasses studied in [3, 14], the X-ray photoelectron spectrum of the LaBS glass does not exhibit splitting of the peaks of the $4f_{5/2}$ and $4f_{7/2}$ states due to the presence of plutonium in two different valence states, even though the spacing between the maxima of the peaks (12.5 eV) almost coincides with that (12.7 eV) for other glasses. The splitting (~ 1.8 eV) of the peaks of the $4f_{5/2}$ and $4f_{7/2}$ states in the spectra of sodium borosilicate glasses with a high iron content (~ 10 wt % in terms of the Fe_2O_3 oxide) indicates the coexistence of the states Pu(IV) and Pu(III) [14]. It should be noted that the formation of Pu(III) can be explained by the reduction of Pu(IV) to Pu(III) as a result of the redox reaction $\text{Fe}^{2+} + \text{Pu}^{4+} = \text{Fe}^{3+} + \text{Pu}^{3+}$ at moderate temperatures of glass melting ($\leq 1250^\circ\text{C}$).

It should also be noted that the binding energy of the $4f_{7/2}$ state of plutonium (table) in the LaBS glass (426.5 eV) nearly coincides with the corresponding energy for the PuO_2 oxide (426.6 eV).

The M–O distances determined using relationships (1) and (2) are averaged for the surface layer of the glass sample. The distance $R_{M-O} = 0.176$ nm, for the most part, reflects the presence of bonds between oxygen and light elements Si–O ($R_{\text{Si-O}} = 0.162$ nm), Al–O ($R_{\text{Al-O}} = 0.174$ nm), and B–O ($R_{\text{B-O}} \approx 0.147$ nm),

whereas the distance $R_{M-O} = 0.191$ nm corresponds to a larger contribution of the Ln–O bonds ($R_{\text{Ln-O}} = 0.22\text{--}0.25$ nm) [18, 19].

CONCLUSIONS

Thus, it has been revealed that the lanthanide borosilicate glass sample prepared at a temperature of 1500°C contains traces of crystalline phases of the britholite type, PuO_2 , and, possibly, pyrochlore. The elemental and ionic quantitative analyses of the surface of the sample were performed using the characteristics of the X-ray photoelectron spectra of the inner electrons in the binding energy range 0–1000 eV. The oxidation states of the ions of the elements in the glass were determined. These oxidation states correspond to the Al^{3+} , La^{3+} , Nd^{3+} , Gd^{3+} , Hf^{4+} , Pu^{4+} , Si^{4+} and Sr^{4+} ions. Taking into account the binding energies of the O 1s electrons for the glass sample under investigation, the lengths of metal–oxygen bonds on the surface of the sample were estimated to be 0.191 and 0.176 nm, which correspond to oxygen binding energies of 531.3 and 532.3 eV, respectively.

ACKNOWLEDGMENTS

We would like to thank S.I. Perevalov, A.G. Ptashkin, and O.I. Stefanovskaya for preparing the glass sample used in our experiments.

This study was supported by the Department of Energy of the United States and the Russian Foundation for Basic Research (project no. 08-03-0031a).

REFERENCES

1. Stefanovsky, S.V., Vudintsev, S.V., Giere, R., and Lumpkin, G.R., Nuclear Waste Forms, in *Energy, Waste, and the Environment: A Geological Perspective (Geological Society Special Publication)*, Gieré, R. and Stille, P., Eds., London: The Geological Society of London, 2004, vol. 236, pp. 37–63.
2. *Review of Excess Weapons Plutonium Disposition LLNL Contract Work in Russia*, Jardine, L.J. and Borosov, G.B., Eds., Livermore: Lawrence Livermore National Laboratory, 2002, UCRL-ID-149341.
3. Veal, B.W., Mundy, J.N., and Lam, D.J., Actinides in Silicate Glasses, in *Handbook on the Physics and Chemistry of the Actinides*, Freeman, A.J. and Lander, G.H., Eds., Amsterdam: Elsevier, 1987, vol. 5, pp. 271–309.
4. Eller, P.G., Jarvinen, G.D., Purson, J.D., Penneman, R.A., Ryan, R.R., Lytle, F.W., and Greeger, R.B., Actinide Valences in Borosilicate Glass, *Radiochim. Acta*, 1985, vol. 39, pp. 17–22.
5. Mesko, M.G., Meaker, T.F., Ramsey, W.G., Marra, J.C., and Peeler, D.K., Optimization of Lanthanide Borosilicate Frit Compositions for the Immobilization of Actinides Using a Plackett–Burman/Simplex Algorithm Design, *Mater. Res. Soc. Symp. Proc.*, 1997, vol. 465, pp. 105–110.

6. Marra, J.C., Crawford, C.L., and Bibler, N.E., *Glass Fabrication and Product Consistency Testing of Lanthanide Borosilicate Frit X Composition for Plutonium Disposition*, Aiken: Savannah River National Laboratory, Department of Energy, Report no. WSRC-STI-2006-00318, 2006.
7. Stefanovsky, S.V., Maslakov, K.I., Teterin, A.Y., Teterin, Y.A., and Marra, J.C., Uranium Speciation in Borosilicate Waste Glass, in *Proceedings of the XXXVI Journées des Actinides, Oxford, United Kingdom, 2006*, Oxford, p. 38.
8. Teterin, Yu.A. and Teterin, A.Yu., Structure of X-Ray Photoelectron Spectra of Lanthanide Compounds, *Usp. Khim.*, 2002, vol. 71, no. 5, pp. 401–504.
9. *Practical Surface Analysis by Auger and X-Ray Photoelectron Spectroscopy*, Briggs, D. and Seah, M., Eds., New York: Wiley, 1983. Translated under the title *Analiz poverkhnosti metodami ozhe- i rentgenovskoi fotoelektronnoi spektroskopii*, Moscow: Mir, 1987.
10. Nefedov, V.I., *Rentgenoelektronnaya spektroskopiya khimicheskikh soedinenii* (X-Ray Photoelectron Spectroscopy of Chemical Compounds), Moscow: Khimiya, 1984 [in Russian].
11. Sosul'nikov, M.I. and Teterin, Yu.A., X-Ray Photoelectron Investigation of Calcium, Strontium, Barium, and Their Oxides, *Dokl. Akad. Nauk SSSR*, 1991, vol. 317, no. 2, pp. 418–421.
12. Teterin, Yu.A. and Teterin, A.Yu., The Structure of X-Ray Photoelectron Spectra of Light Actinide Compounds, *Usp. Khim.*, 2004, vol. 73, no. 6, pp. 588–631.
13. Ewing, R.C., Weber, W.J., and Lutze, W., Crystalline Ceramics: Waste Forms for the Disposal of Weapons Plutonium, in *Disposal of Weapons Plutonium*, Merz, E.R. and Walter, C.E., Eds., Dordrecht, The Netherlands: Kluwer, 1996, pp. 65–83.
14. Karin, D.P., Lam, D.J., Diamond, H., Friedman, A.M., Coles, D.G., and Bazan, F., XPS Valence State Determination of Np and Pu in Multicomponent Borosilicate Glass and Application to Leached 76–68 Waste Glass Surface, *Mater. Res. Soc. Symp. Proc.*, 1982, vol. 6, pp. 67–73.
15. Buck, E.C., Ebbinghaus, B., Bakel, A.J., and Bates, J.K., Characterization of a Plutonium-Bearing Zirconolite-Rich Synroc, *Mater. Res. Soc. Symp. Proc.*, 1997, vol. 465, pp. 1259–1266.
16. Hess, N.J., Weber, W.J., and Conradson, S.D., U and Pu L_{III} XAFS of Pu-Doped Glass and Ceramic Waste Forms, *J. Alloys Compd.*, 1998, vols. 271–273, pp. 240–243.
17. Hess, N.J., Weber, W.J., and Conradson, S.D., X-Ray Absorption Fine Structure of Aged, Pu-Doped Glass and Ceramic Waste Forms, *Mater. Res. Soc. Symp. Proc.*, 1998, vol. 506, pp. 169–176.
18. Shannon, R.D., Revised Effective Ionic Radii and Systematic Studies of Interatomic Distances in Halides and Chalcogenides, *Acta Crystallogr., Sect. A: Cryst. Phys., Diffraction, Theor. Gen. Crystallogr.*, 1976, vol. 32, pp. 751–767.
19. Larson, E.M., Lytle, F.W., Eller, P.G., Greeger, R.B., and Eastman, M.P., XAS Study of Lanthanide Ion Speciation in Borosilicate Glass, *J. Non-Cryst. Solids*, 1990, vol. 116, pp. 57–62.